PCCP

RSC Publishing

PAPER

View Article Online
View Journal

Cite this: DOI: 10.1039/c2cp43098c

Sodium-doping as a reference to study the influence of intracluster chemistry on the fragmentation of weakly-bound clusters upon vacuum ultraviolet photoionization

Jessica H. Litman, Bruce L. Yoder, Bernhard Schläppi and Ruth Signorell*

The fragmentation of methanol, water, dimethyl ether, and acetic acid clusters upon photoionization with a single vacuum ultraviolet (VUV) photon of 10.1 eV, 13.3 eV, or 17.5 eV energy is studied with mass spectrometry. The sodium-doping method is used as an independent approximate measure of the original cluster size distribution providing information on the degree of fragmentation upon VUV ionization. The experimental results show strong fragmentation for $(CH_3)_2O$ and CH_3CO_2H clusters but minor fragmentation for H_2O and CH_3OH clusters. The pronounced cluster decay for $(CH_3)_2O$ and CH_3CO_2H is explained by additional intracluster chain reactions that occur after the initial fast proton transfer in the ionic clusters, *i.e.* the decay of $(CH_3)_2O$ molecules into H_2, CO, and CH_4 catalyzed by the methoxymethyl radical, and the decay of CH_3CO_2H molecules into CO_2 and CH_4 catalyzed by the acetyloxy radical. The absence of equivalent reaction cycles in ionic H_2O and CH_3OH clusters after the fast proton transfer is consistent with the much less pronounced cluster fragmentation observed upon VUV ionization. The study shows that VUV photoionization even at threshold cannot in general be considered a soft ionization method for weakly-bound clusters, largely because of potential intracluster reaction.

Received 5th September 2012,
Accepted 20th November 2012

DOI: 10.1039/c2cp43098c

www.rsc.org/pccp

1. Introduction

The study of intracluster reactions in weakly-bound cluster cations has attracted a lot of attention in the past (Jena and Castleman Jr.[1] and references therein). The better understanding of solvation effects on reactions was a major motivation behind many of these investigations. Typically the neutral clusters were generated in a molecular beam apparatus and the ionic chemistry was studied after ionization (single photon (SPI), multiphoton (MPI), electron ionization (EI), chemical ionization) by mass spectrometry. For the substances studied in the present work – methanol (MeOH, CH_3OH), water (H_2O), dimethyl ether (DME, $(CH_3)_2O$), and acetic acid (HAc, CH_3CO_2H) – all these studies consistently report that after ionization protonated cluster ions dominate the mass spectra (ref. 2–5 and references therein). These protonated species are produced by fast proton transfer reactions and the supposedly subsequent loss of the formed radical from the clusters.

The influence of intracluster reactions on the fragmentation of ionic clusters has been recognized, but it has proven to be difficult to study experimentally (see comments in Dong *et al.*[2]). The major reason is the lack of independent experimental information on the size distribution of the original clusters before ionization. The degree of fragmentation is usually inferred from the size distribution of parent and daughter ions recorded in the mass spectra after SPI, MPI, or EI. Since fragmentation depends on various factors, *e.g.* on the ionization method and the excess energy available, it can have many origins that are difficult to disentangle. It has been shown that SPI is in general superior to MPI and EI in this respect (see for example Dong *et al.*[2] and references therein). However, even with SPI an independent reference of the original cluster size distribution is missing.

We have recently demonstrated that single atom Na-doping of the clusters with subsequent ionization of the Na with a UV laser at 266 nm followed by mass spectrometric detection (referred to as ''Na-doping'' in the following) seems a viable method to measure original size distributions (except for corrections for the overall detection efficiency as discussed below) of large weakly-bound clusters and ultrafine aerosol particles largely destruction-free.[6] Compared with other ionization methods, Na-doping turns out to be an ultrasoft sizing method for such weakly-bound molecular aggregates generated

Department of Chemistry, University of British Columbia, 2036 Main Mall, Vancouver, British Columbia V6T 1Z1, Canada. E-mail: signorell@chem.ubc.ca

by supersonic expansions.[6–8] There are several reasons why Na-doping is softer for these systems than other methods. The major reason is the low ionization energy of Na-doped clusters (<5 eV), which typically lies far below the ionization energy of the undoped clusters (>10 eV). By choosing photons with energies below 5 eV, one can ionize Na-doped clusters without ionizing the molecules of the clusters themselves. For this reason, one avoids the problem with ionic chemistry that can happen after direct ionization of undoped clusters and consequently one also avoids the resulting cluster decay. Additionally, by choosing suitable photon energies below 5 eV one can minimize the excess energy relative to the ionization energy of the Na-doped clusters, which can help to further minimize fragmentation. Our previous studies reveal that during the whole detection process using the Na-doping method typically a few molecules are lost from a cluster.[6,9] Compared with the overall number of molecules in a large cluster or ultrafine aerosol this is almost negligible and therefore makes Na-doping an ultrasoft sizing method. We would also like to mention here that Na-doping is not a good method for sizing small clusters (dimers, trimers, *etc.*) because on average the original cluster loses a few molecules during the whole detection step.[6,9] For general properties of weakly-bound Na-doped clusters we refer to the extensive work published by Buck and co-workers and Hertel and co-workers (Cwiklik *et al.*,[10] Liu *et al.*[11] and references therein).

In the present contribution, we use Na-doping as a reference method to obtain independent approximate information of the original cluster size distribution in order to study the influence of ionic chemistry upon direct photoionization of various weakly-bound clusters with a single vacuum ultraviolet (VUV) photon. The VUV mass spectra were recorded at three different photon energies. This includes measurements just above the ionization threshold, which is often considered to be a soft ionization method that avoids major cluster fragmentation. Our results for DME and HAc clusters in Section 3.1, however, demonstrate that this is not always the case. The comparison with the Na-doping method shows that even threshold SPI can result in substantial cluster decay. We believe that intracluster chemistry is the major reason for cluster fragmentation in these cases. Possible reaction pathways that could explain the observed cluster decay are provided in Section 3.2. The absence of analogous favourable reaction pathways in MeOH and H_2O cluster ions explains why fragmentation after VUV ionization is much less pronounced for these two examples (Section 3.3).

2. Experiment and computation

2.1 Experiment

The experimental setup is shown in Fig. 1 (see Forysinski *et al.*[9,12] for similar setup). Fig. 2 provides a sketch of the two different types of experiments performed on each cluster beam studied: Experiment 1 determines the original cluster size distribution with the Na-doping method (reference for original cluster size), while Experiment 2 is the actual VUV single photon experiment. The comparison of the VUV mass spectrum

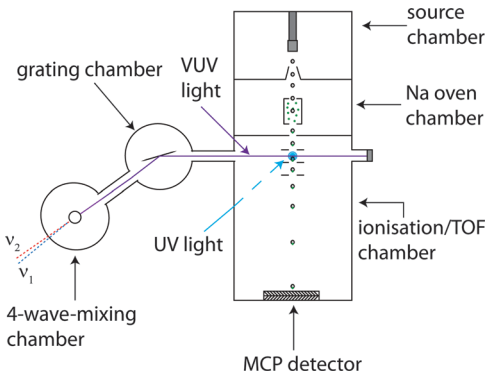

Fig. 1 Sketch of the experimental setup consisting of the cluster beam apparatus with the Na-oven and the tabletop VUV laser (see Section 2.1).

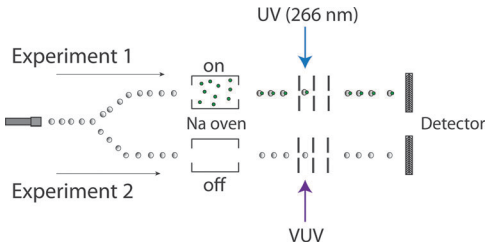

Fig. 2 Experiment 1: determination of the original cluster size distribution with the Na-doping method (Na oven on; photoionization of Na-doped clusters with UV light at 4.66 eV). Experiment 2: actual VUV single photon experiment (Na oven off; photoionization of undoped clusters with VUV light at 10.1 eV, 13.3 eV, or 17.5 eV).

with the UV Na-doping mass spectrum allows us to determine the degree of cluster fragmentation induced by VUV light.

The neutral clusters of the respective substances were formed in vacuum in the source chamber (Fig. 1) either by neat or He-seeded pulsed (10 Hz) supersonic expansions (Parker Hannifin) at total backing pressures between 1 and 5 bars. The sample gases were prepared in a cylinder containing a desiccant to reduce water impurities. The following substances were used: He (Praxair, >99.999%), MeOH (Fisher Scientific, >99.9%), H_2O (Cayman Chemical Company, R > 18 MΩ, total organic contaminants <10 ppb), DME (Specialty Gases of America, >99.7%), and HAc (Fisher Scientific, glacial, >99.7%). The cluster beam first entered the Na-oven chamber through a 1 mm skimmer. After passing the Na-oven the clusters entered the ionization/TOF chamber through a 4 mm hole to be ionized either with UV light in the case of Na-doped clusters or with VUV light in the case of undoped clusters (see below). The ions were accelerated in a three-plate Wiley–McLaren type extractor and detected with a microchannel plate (MCP) detector at the end of the 50 cm long linear time-of flight tube. The pressure during operation in the various chambers was kept below $\sim 5 \times 10^{-4}$ mbar (source chamber), $\sim 5 \times 10^{-7}$ mbar (Na-oven chamber), and $\sim 1 \times 10^{-7}$ mbar (ionization/TOF chamber), respectively. The interaction of the UV or VUV light with the cluster beam occurred between the first and second plate of the extractor. Since at low extraction voltages heavier ions could be

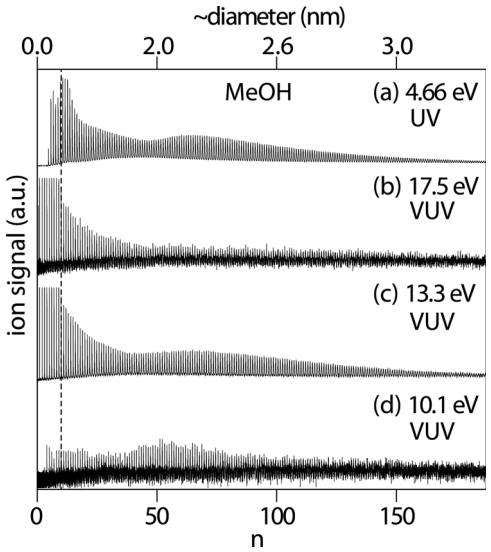

Fig. 3 (a) UV mass spectrum of Na-doped MeOH clusters recorded at a UV photon energy of 4.66 eV. (b) VUV mass spectrum of the corresponding undoped MeOH clusters recorded at a photon energy of 17.5 eV. (c) VUV mass spectrum of the corresponding undoped MeOH clusters recorded at a photon energy of 13.3 eV. (d) VUV mass spectrum of the corresponding undoped MeOH clusters recorded at a photon energy of 10.1 eV. The mass spectra are shown as a function of the cluster diameter (abscissa on top) and the number of molecules, *n*, per cluster (abscissa at the bottom). *n* = 50 corresponds to a mass of 1600 *m*/*z*. All mass spectra were recorded with an extraction voltage of 14 keV.

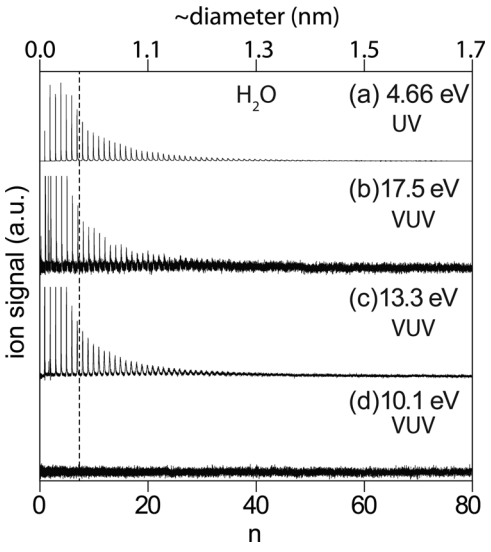

Fig. 4 The same as in Fig. 3 but for H_2O clusters. *n* = 20 corresponds to a mass of 360 *m*/*z*. All mass spectra were recorded with an extraction voltage of 5 keV.

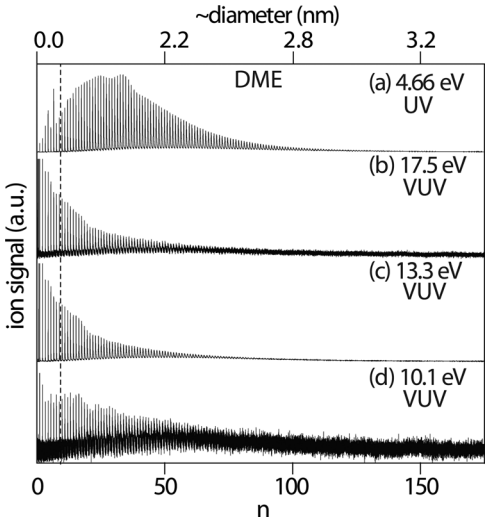

Fig. 5 The same as in Fig. 3 but for DME clusters. *n* = 50 corresponds to a mass of 2300 *m*/*z*. All mass spectra were recorded with an extraction voltage of 11 keV.

detected at the MCP with lower efficiency than lighter ions we have recorded mass spectra at a range of extraction voltages between 1 and 14 keV for all substances. We have only considered mass spectra for which the extraction voltages were high enough so that ions of different masses were detected with similar efficiencies. More importantly, the UV spectrum and all corresponding VUV spectra we compare for a certain substance were recorded with the same extraction voltage; *i.e.* ions of a certain mass are detected at the MCP with the same efficiency in the UV and the VUV mass spectra. Values for extraction voltages used for the spectra displayed in Fig. 3–6 are given in the respective figure captions. The mass resolving power of the current setup is $\sim 380\ m/\Delta m$ (FWHM) at 2000 *m*/z. We present our results here for medium-sized aggregates (radius < 1.5 nm) due to the limited resolving power. Nevertheless, the conclusions we draw should remain equally valid for larger systems; *e.g.* ultrafine aerosols.

As Fig. 2 shows, all original cluster size distributions were first measured with the Na-doping method (Experiment 1) before the VUV experiment (Experiment 2) was performed. Each cluster was doped with a single Na after passing through the 44 mm long Na oven, which was kept at a temperature of 480 K. (Multiple Na-doping is negligible under these conditions as experimentally confirmed by the lack of any multiple doped ion signals in the mass spectra.) The Na-doped clusters were then ionized with a single UV photon of 4.66 eV energy. Typically, UV ionization was performed with energies of 0.5 to 2.5 mJ per pulse (unfocused, spot size ~ 2 mm) provided by a Nd:YAG (Quantel Ultra 50) with 8 ns pulse duration at a repetition rate of 10 Hz. Except for the addition of a Na atom the Na-doping method leaves the sizes of the original clusters virtually intact because only few molecules are evaporated from the clusters and their chemical composition does not change.[6,9] However, as discussed in ref. 6, 9 the relative abundance of clusters of different masses in a size distribution can be modified by the Na-doping method, because the Na-capture efficiency, the Na-sticking efficiency, and the detection efficiency at the MCP in general depend on the size. The MCP efficiency does not pose any issue in the present work as explained in the previous paragraph. For very small clusters (dimers, trimers, *etc.*), the Na-capture efficiency and the Na-sticking efficiency (*i.e.* the collision complex lifetime) depend very strongly on the specific cluster type and are typically small (see ref. 9). For this reason, we exclude the small cluster region in Fig. 3–6

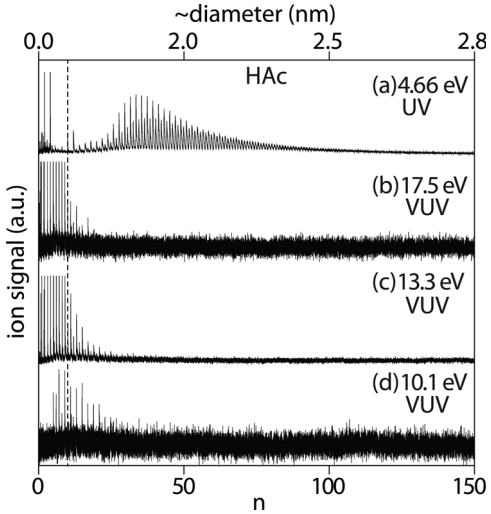

Fig. 6 The same as in Fig. 3 but for HAc clusters. n = 50 corresponds to a mass of 3000 m/z. All mass spectra were recorded with an extraction voltage of 5 keV.

(approximately the regions to the left of the dashed lines) from any comparison with VUV mass spectra in the present work. For larger clusters, the sticking efficiency is determined by local processes and is thus size-independent (see ref. 6). The Na-capture efficiency of the larger clusters is determined by their geometric cross sections, *i.e.* it scales with r^2, where r is the radius of the aggregate.[6] Corresponding corrections for the present spectra are minor and do not affect any of our arguments. We therefore show uncorrected spectra only. The size distributions determined with the Na-doping method (Experiment 1) in the region to the right of the dashed line in Fig. 3–6 can therefore be taken as approximations of the original neutral cluster size distributions and as a reference to study cluster decay upon VUV ionization (Experiment 2).

A custom-built pulsed (10 Hz) tunable VUV laser light source[12] was used for the VUV experiments (Experiment 2). Three different photon energies (10.1 eV, 13.3 eV, and 17.5 eV) were used in the present study. The light was generated in the VUV chamber by resonance-enhanced 2-colour 4-wave-mixing in a pulsed jet of Kr gas. The Kr two-photon resonance at 94092.862 cm^{-1} was pumped by the tripled output (ν_1) of a dye laser (Sirah: Cobra-stretch SL). The third photon necessary to generate 17.5 eV light came from the same dye laser, while a second dye laser (Sirah: Cobra-stretch SL) was required to provide the third photon (ν_2) for the generation of 13.3 eV and 10.1 eV light. Both dye lasers were pumped by the output of a single Nd:YAG (Continuum Powerlite PR 9010) with $\sim$8 ns pulse duration. The resulting VUV photon flux was estimated to be in the nJ per pulse range (defocused, spot size $\sim$1.5–2 mm). The 266 nm UV laser and the VUV laser probed the same spatial and temporal section of the pulsed molecular beam. UV laser, VUV laser, and molecular beams intersected at 90 degrees (see Fig. 1).

2.2 Computation

The approximate enthalpies of reactions used in Section 3 were calculated from the enthalpies of formation of gas phase molecules, radicals, and cations found in the literature.[13–18] All values refer to gas phase species at standard temperature (298 K) and can therefore serve only as a rough guide of the enthalpy balance in the molecular aggregates we are interested in. Their pre-ionization temperature is not known (presumably $<$200 K for all conditions (neat, seeded in He)), but we expect the average thermal energy per degree of freedom to be insignificant relative to the energy balance of the processes taking place after ionization. The use of gas phase values represents a more serious approximation, since both reactant and product species experience significant intermolecular interactions (often involving hydrogen bonds). The interaction energies range from several tenths of an electron volt for neutral species up to more than one electron volt for ionic species. We have taken this aspect into account in our discussion below. To estimate the number of molecules that could be evaporated from a cluster ion for a certain amount of energy available we use bulk enthalpies of vaporization at room temperature taken from the literature.[13] This corresponds to an upper limit for the number of evaporated molecules since the dissociation energies for single molecules from small charged clusters are expected to be larger or approximately equal to the bulk vaporization enthalpies (see data for charged H_2O, MeOH, DME clusters[2,3,19–21]), and cluster temperatures lie below room temperature. Note that this is consistent with the use of vaporization enthalpies (instead of sublimation enthalpies) as we do not know whether the clusters are liquid-like or solid-like. We consistently use the adiabatic ionization energies of the gas phase monomers for all estimates[22–25] since most values for clusters of different size are not available. Some values for ionization energies and appearance energies of dimers, larger clusters, and bulk can be found in ref. 3, 26–29. Note that liquid phase values can be more than 1 eV lower than gas phase values.

Density functional calculations were carried out with Gaussian 09 (ref. 30) to derive enthalpies and barriers of some selected compounds. We employed the B3LYP functional together with the 6-311++G(3df,2p) basis set. This split-valence basis set is of triple zeta quality and includes polarization and diffuse functions, which allow for a balanced treatment of radicals, radical ions, and neutrals as well as hydrogen bonds. We have checked the sensitivity of the results to the size basis set and found no qualitative difference for smaller basis sets. We did not apply any corrections for basis set superposition errors, which should be negligible for our purposes. Although B3LYP builds on a local density functional, its use should be justified here since the systems we study are dominated by covalent and electrostatic interactions as confirmed by the comparison with MP2 and CCSD(T) calculations in select cases (not reported here). Using the electronic energies and (unscaled) harmonic frequencies calculated for equilibrium and transition state structures we derived the values for reaction enthalpies (at 0 K) and barrier heights (zero point corrected) reported in Table 1.

3. Results

3.1 Single photon VUV ionization *versus* Na-doping

Fig. 3–6 compare UV mass spectra of large Na-doped clusters (top traces) with the VUV mass spectra (lower traces) of the

Table 1 Theoretical barrier heights $\Delta E^{\ddagger}$ (including zero point correction) and standard reaction enthalpies $\Delta_r H^0_{0K}$ (at 0 K) relative to reactants calculated at the B3LYP/6-311++G(3df,2p) level

Reactants	Products	$\Delta E^{\ddagger}$/ eV	$\Delta_r H^0_{0K}$/ eV	$\Delta_r H^{0\,a}$/ eV (exp.)
$(CH_3)_2O$	$CH_4 + CH_2O$		−0.16	+0.01
CH_2O	$CO + H_2$		+0.03	−0.02
$(CH_3)_2O^+ + (CH_3)_2O$	$CH_3OCH_2 + HO^+(CH_3)_2$	[b,d]	−0.15	−0.37
CH_3OCH_2	$CH_3 + CH_2O$	+0.96	+0.28	+0.29
$CH_3OCH_2\cdots HO^+(CH_3)_2$	$CH_3 + CH_2O\cdots HO^+(CH_3)_2$	+0.77	+0.28	
$CH_3 + CH_2O$	$CH_4 + HCO$	+0.25	−0.74	−0.71
HCO	$CO + H$	[c]	+0.87	+0.66
$CH_3 + (CH_3)_2O$	$CH_4 + CH_3OCH_2$	+0.44	−0.44	−0.28
$HCO + (CH_3)_2O$	$CH_2O + CH_3OCH_2$	+0.71	+0.30	+0.43
$H + (CH_3)_2O$	$H_2 + CH_3OCH_2$	+0.09	−0.53	−0.26
$CH_3CO_2H^+ + CH_3CO_2H$	$CH_3CO_2 + CH_3CO_2H_2^+$	[b]	−0.48	−0.78
CH_3CO_2	$CH_3 + CO_2$	[b]	−0.63	−0.22
$CH_3 + CH_3CO_2H$	$CH_4 + CH_3CO_2$	+0.40	+0.03	−0.15

[a] Experimental values from standard enthalpies of formation (see Section 3.2). [b] No barrier. [c] No barrier for the reverse reaction. [d] The binding energy of the dimer ion is 1.15 eV.

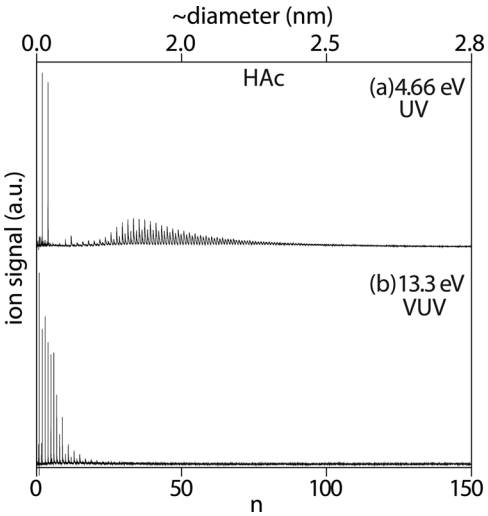

Fig. 7 The same HAc spectra (a) as in Fig. 6a and (b) as in Fig. 6c. All mass peaks to the left of the dashed line in Fig. 6 are displayed here with their true intensities, *i.e.* they are not intentionally cut as in Fig. 6 (see text).

corresponding undoped clusters for four different substances. The UV spectrum and the VUV spectra (at 17.5 and 13.3 eV) are scaled to the mass peaks $n = 30$, $n = 8$, $n = 6$, $n = 12$, respectively. Please note that UV and VUV spectra in the region to the left of the dashed lines cannot be compared because in this size range the detection efficiency of the Na-doping method strongly depends on the specific cluster type (see discussion in Section 2.1). The efficiency is in general small here and decreases with decreasing cluster size (goes to zero for the monomer). We would also like to emphasize that the mass peaks in the VUV spectra at 17.5 and 13.3 eV (and the two low mass peaks in the UV spectrum of Fig. 6a) are not saturated in this region. We have intentionally cut some of them in Fig. 3–6 because of this efficiency issue to more clearly display the region to the right of the dashed lines, which will be important for the comparisons and arguments below. The true intensity of the cut mass peaks is roughly 2–3 times higher. Fig. 7 shows as an example the UV and the 13.3 eV VUV spectrum of HAc with mass peaks representing the true intensities.

Both methods – VUV mass spectrometry of undoped clusters and UV mass spectrometry of Na-doped clusters – probe the same original cluster size distribution and thus should result in similar mass spectra (in the region to the right of the dashed lines) since both methods are considered soft ionization methods. This is approximately the case for the MeOH clusters and for the H_2O clusters. The UV mass spectrum of Na-doped MeOH clusters (Fig. 3a) looks similar to the VUV mass spectrum of undoped MeOH clusters recorded at 13.3 eV (Fig. 3c). It is also similar to the VUV mass spectrum recorded at 17.5 eV (Fig. 3b), although this might be difficult to see because of the low signal to noise (note that cluster peaks with more than 150 molecules are visible in the 17.5 eV spectrum). We display the 10.1 eV mass spectrum in trace (d) for completeness only. It cannot be compared directly with the UV mass spectrum in trace (a) since the photon energy of 10.1 eV lies 0.75 eV below the adiabatic ionization energy of MeOH monomer (10.85 eV (ref. 22)). Under such conditions the ionization cross sections tend to be very low or even vanish for some cluster sizes so that no statement can be made about their relative abundance. With respect to fragmentation, the behaviour of H_2O clusters (Fig. 4) is similar to that of methanol clusters. As before we do not find any major difference between the mass spectra obtained by the Na-doping method (Fig. 4a) and those measured with direct VUV ionization (Fig. 4b and c). Note that no mass peaks are visible in the 10.1 eV spectrum in trace (d) because this energy lies below the ionization energies of all clusters (adiabatic ionization energy of the monomer is 12.62 eV (ref. 23)).

The situation is completely different for DME clusters (Fig. 5) and for HAc clusters (Fig. 6) as we had qualitatively demonstrated before.[6] While the UV mass spectra (traces (a)) show intact cluster size distributions, the VUV mass spectra show size distributions that one would expect after extensive cluster fragmentation, *i.e.* the information about the original size distribution is lost. For both, DME and HAc, this is true almost independently of the excess energy of the VUV photon relative to the monomer ionization energy (traces (b)–(d)). Note that 10.1 eV lies just above the monomer ionization energy of DME (10.025 eV (ref. 24)) but below the monomer ionization energy of HAc (10.65 eV (ref. 25)), *i.e.* for both substances in a range where ionization cross sections for clusters are low or vanish and strongly depend on cluster size. For the example of DME, the excess energies relative to the monomer ionization energy are ~0.1 eV for the 10.1 eV spectrum, ~3.3 eV for the 13.3 eV spectrum, and ~7.5 eV for the 17.5 eV. Evidently, the excess energy is not the major driving force of the cluster destruction, which is pervasive in the VUV mass spectra of DME and HAc even for threshold ionization. The mere presence of the molecular ion must be the key factor. As pointed out previously[6] this is a hint that the destruction of the clusters upon direct VUV ionization might be the result of intracluster ion chemistry, which cannot occur upon UV ionization of the Na-doped clusters.

More evidence for the involvement of ionic chemistry comes from the inspection of the masses of the different clusters. All VUV mass spectra are dominated by mass peaks that correspond to protonated clusters with the general formula $(M)_n\ H^+$ (M = MeOH, H_2O, DME, HAc; n is the number of molecules M in the cluster). The dominance of protonated species after single photon, multiphoton, and electron ionization has been observed before and is well documented in the literature (ref. 2–5 and references therein). It is explained by fast intracluster proton transfer following ionization according to eqn (1).

$$(M)_n + h\nu \rightarrow (M)_{n-1}\ H^+ + R + e^- \qquad (1)$$

where R is the neutral radical resulting from H abstraction, *i.e.* the methoxy radical (CH_3O), the hydroxyl radical (OH), the methoxymethyl radical (CH_3OCH_2), and the acetyloxy radical (CH_3COO), respectively. Fig. 8 demonstrates for the example of a $(MeOH)_{10}$ cluster that this proton transfer does not take place for the Na-doping method (traces (a) and (b)). The mass peak in trace (a) corresponds to an intact cluster ion with one Na attached. Shifting this spectrum by −23 m/z (mass of Na) (trace b) the peak lies one mass unit below the mass peak of the corresponding protonated cluster in the VUV spectrum in trace (c).

Model calculation for dimers show that the proton transfer reaction (eqn (1)) is barrierless and therefore clearly very fast, but as argued in the following Section 3.2, the proton transfer alone cannot account for the striking differences between Na-doping and VUV for DME (Fig. 5) and HAc (Fig. 6). We believe that after the proton transfer additional intracluster reactions must take place that result in the shrinking of the original clusters, but which are not otherwise visible in the mass spectra. Since the VUV mass spectra predominantly show protonated clusters, those intracluster reactions must form small neutral fragments that can easily leave the cluster.

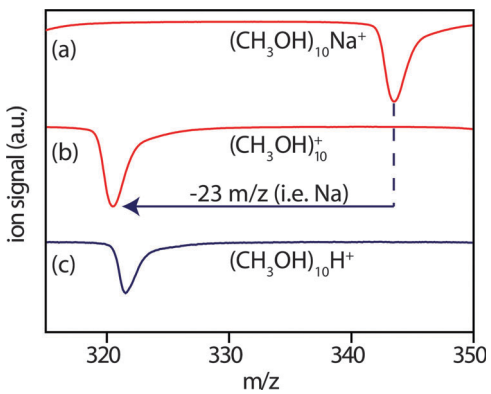

Fig. 8 Mass spectra in the region of the $(MeOH)_{10}$ cluster. (a) Recorded after Na-doping and UV excitation with 4.66 eV. Mass peak corresponds to $(MeOH)_{10}Na^+$. (b) The same as in trace (a) but shifted to lower mass by −23 mass units (mass of Na). Mass peak corresponds to $(MeOH)_{10}^+$. (c) Recorded after VUV excitation at 13.3 eV. Mass peak corresponds to the protonated $(MeOH)_{10}H^+$ cluster.

If the fragments remained in the cluster they would give rise to major mass peaks other than those corresponding to the protonated species. Since this is not the case the protonated clusters initially formed after ionization lose the molecular radical R and shrink without further changing their chemical composition. This is only possible either through very exothermic reactions or through exothermic or essentially thermo-neutral chain reactions. As outlined below, such processes can be formulated for DME and HAc, but not for H_2O and MeOH where analogous reactions do not exists or would be strongly endothermic, respectively. In the latter two cases, the minor differences found between Na-doping and VUV mass spectra (Fig. 3 and Fig. 4b and c) are likely the result of the fast proton transfer and the ensuing structural reorganization of the solvation shell.

3.2 Case I: extensive cluster decay after VUV ionization

DME clusters. Eqn (2)–(4) provide possible reactions and mechanisms for DME cluster cations that fulfill all the conditions listed above for intracluster reactions capable of destructing the cluster. The intracluster proton transfer (eqn (2)) results in a methoxymethyl radical. It can either leave the cluster or catalyze the decay of DME molecules into neutral fragments (eqn (3) and (4)).

$$(CH_3)_2O^+ + (CH_3)_2O \rightarrow CH_3OCH_2 + (CH_3)_2OH^+ \quad \Delta_rH \sim -0.37\ \text{eV} \qquad (2)$$

$$(CH_3)_2O = CH_2O + CH_4 \quad \Delta_rH \sim +0.01\ \text{eV} \qquad (3)$$

$$(CH_3)_2O = H_2 + CO + CH_4 \quad \Delta_rH \sim -0.01\ \text{eV} \qquad (4)$$

The proton transfer (eqn (2)) happens once in a cluster with a reaction enthalpy of roughly ∼36 kJ mol^{-1}. From calculations for various configurations for DME-dimer and its ion we estimate a reorganization energy of −(10–20) kJ mol^{-1} (−(0.1–0.2) eV) associated with the ionization and the subsequent proton transfer. Assuming an enthalpy of vaporization of $\Delta_{vap}H$ ∼ 19.3 kJ mol^{-1} the available energy would on average suffice to evaporate at most three molecules per cluster. This can not explain the substantial decay of the clusters after VUV excitation visible in traces (b) to (d) of Fig. 5 compared with the intact Na-doped clusters in trace (a). (As noted above the thermal energy of the cluster is insignificant in this context.) The essentially thermoneutral radical catalyzed reactions (3) and (4), by contrast, can occur many times and in this way break up the original cluster. In the neutral molecule, the fragmentation of DME into smaller molecules is kinetically hindered, but in the ionic cluster the formation of the methoxymethyl radical opens up a catalytic cycle that can destroy the original cluster through successive formation and evaporation of methane and either formaldehyde or hydrogen and carbon monoxide. The following mechanisms appear plausible for these chain reactions:

$$CH_3OCH_2 \rightarrow CH_3 + CH_2O \quad \Delta_rH \sim +0.29\ \text{eV} \qquad (3a)$$

$$CH_3 + (CH_3)_2O \rightarrow CH_4 + CH_3OCH_2 \quad \Delta_rH \sim -0.28\ \text{eV} \qquad (3b)$$

or

$$CH_3OCH_2 \rightarrow CH_3\cdots CH_2O \rightarrow CH_4 + HCO \quad \Delta_rH \sim -0.42 \text{ eV} \quad (4a)$$

$$HCO \rightarrow CO + H \quad \Delta_rH \sim +0.66 \text{ eV} \quad (4b)$$

$$H + (CH_3)_2O \rightarrow H_2 + CH_3OCH_2 \quad \Delta_rH \sim -0.26 \text{ eV} \quad (4c)$$

In both cases the initial step involves breaking the C–O bond, as there does not appear to exist a separate concerted path for the dissociative 1,3-H shift (eqn (4a)). We calculate a relatively high barrier in the isolated radical of almost 100 kJ mol^{-1} (see Table 1). This would appear prohibitive for a thermal reaction, but in the cluster the methoxymethyl radical is probably formed with substantial internal excitation both in the initial proton transfer (eqn (2)) and in the reaction cycles (eqn (3a) and (3b) or (4a)–(4c)). As long as the subsequent steps are fast enough this energy will remain available to drive many cycles before it eventually dissipates away from the area where the reaction takes place. This condition is clearly fulfilled as all subsequent steps have barriers significantly below that of the initial C–O bond breaking. Moreover, the barrier is presumably reduced in the vicinity of the ion. The reduction by about 20 kJ mol^{-1} calculated in the ionic dimer (see Table 1) can serve as an indication for the order of magnitude of this effect. There will also be cage effects that prevent – or at least slow down – the escape of small reactive intermediates (CH_3, HCO, H) from the reaction centre. This might even open up a direct concerted mechanism for the dissociative 1,3-H shift (eqn (4a)). In any case we expect this reaction pathway (eqn (4a)–(4c)) to be the dominant one, because we calculate a significantly lower barrier for the reaction of CH_3 radical with formaldehyde (2nd part of eqn (4a)) than with DME (eqn (3b)) (see Table 1). The intermediate formyl radical could in principle react directly with DME to form formaldehyde (eqn (4d))

$$HCO + (CH_3)_2O \rightarrow CH_2O + CH_3OCH_2 \quad \Delta_rH \sim +0.43 \text{ eV} \quad (4d)$$

This would lead to the same products as the first reaction pathway (eqn (3a) and (3b)). However, we still think that the HCO radical decays according to (eqn (4b)) before it can abstract an H atom from DME. According to our calculations the dissociation of HCO is barrierless. Even though the dissociation energy (0.66 eV) is not significantly lower than the barrier height calculated for eqn (4d) (0.71 eV, Table 1) it should still be much faster since HCO carries significant excess energy from its formation (eqn (4a)). Under such conditions the activation entropy strongly favours the formation of an atomic and a diatomic fragment over the simple H atom transfer of eqn (4d). This line of argument is also consistent with the fact that the VUV photoionization mass spectra do not show any peaks that would correspond to cluster fragments containing CH_2O, which is not a particularly volatile substance at the presumed temperatures of the clusters in the molecular beam. If formaldehyde were formed in any significant amounts some of it should remain in the ionic cluster fragments. CH_4, H_2 and CO, by contrast are very volatile and do not form any hydrogen bonds with DME or DME ion, so that it is plausible for them to leave the cluster quickly.

Further support for the dominance of reaction (4a) comes from decomposition studies of the methoxymethyl radical in a solid argon matrix.[31] The argon matrix provides a monomer environment similar to the gas phase but with a cage effect similar to the clusters. While CH_3 and CH_2O (eqn (3a)) are proposed to be the major decomposition products of the methoxymethyl radical in the gas phase (ref. 31–34 and references therein) it decomposes into CH_4 and HCO (eqn (4a)) in the argon matrix.[31] The new pathway in the matrix is attributed to the cage effect by an argument similar to that made above for the clusters, which supports the dominance of step (4a) over step (3a) in the cluster environment. The subsequent steps, *i.e.* eqn (3b) and (4c) are unlikely to take place in the matrix and gas phase, respectively, because in these ''monomer environments'' no other DME molecules are close enough to react.

We would like to stress again that the VUV mass spectra taken at 10.1 eV, 13.3 eV, and 17.5 eV in Fig. 5 look almost identical, which indicates that the photon excess energy does not play the important role for the cluster shrinking in contrast to the ionic chemistry discussed above. Higher electronic states of the DME ion that could potentially open other decay channels are in principle accessible at 13.3 eV and 17.5 eV.[24] However, such alternative channels are either not important for DME or have the same effect on cluster shrinking. Similarly as for DME clusters, we found also for HAc the intracluster chemistry to play the dominant role for the cluster decay while the excess energy seems to be of minor importance (Fig. 6).

HAc clusters. An equivalent explanation for the extensive cluster decay of the HAc clusters after VUV ionization (Fig. 6) is summarized in eqn (5) and (6). The proton transfer in eqn (5) is fast and releases about 75 kJ mol^{-1} into the cluster, but given the enthalpy of vaporization of $\Delta_{vap}H$ = 51.6 kJ mol^{-1} it cannot explain the cluster decay simply by evaporation of HAc molecules (on average 1–2 molecules) from the clusters.

$$CH_3CO_2H^+ + CH_3CO_2H \rightarrow CH_3CO_2 + CH_3CO_2H_2^+ \quad \Delta_rH \sim -0.78 \text{ eV} \quad (5)$$

$$CH_3CO_2H = CO_2 + CH_4 \quad \Delta_rH \sim -0.37 \text{ eV} \quad (6)$$

The acetyloxy radical formed in reaction (5), however, can catalyze the decay of HAc into carbon dioxide and methane (eqn (6)), which can easily evaporate from the cluster. This chain reaction can happen many times and since each cycle releases 36 kJ mol^{-1} it has the capacity to self-propagate and/or to evaporate HAc molecules from the cluster.

$$CH_3CO_2 \rightarrow CO_2 + CH_3 \quad \Delta_rH \sim -0.22 \text{ eV} \quad (6a)$$

$$CH_3 + CH_3CO_2H \rightarrow CH_4 + CH_3CO_2 \quad \Delta_rH \sim -0.15 \text{ eV} \quad (6b)$$

The first step of the cycle (eqn (6a)) is barrierless (see Table 1) and therefore very fast, as has been observed for acyloxy radicals in general.[14–16] For the second step, we calculate a barrier of about 39 kJ mol^{-1}, which is easily overcome by the available energy. The fragmentation of HAc into carbon

dioxide and methane through this catalytic cycle (eqn (6a) and (6b)) is therefore expected to be very fast.

To obtain final evidence for the reactions proposed, we tried to detect the neutral reaction products with REMPI experiments. For CO_2 (eqn (6)) we employed a 3 + 1 REMPI scheme with ν_3 = 326.40 nm light after VUV excitation with 17.5 eV. This attempt was unfortunately not successful. To avoid the formation of CO_2^+ (and CO^+) by the ν_3 laser alone its power had to be reduced so much that the sensitivity for REMPI on CO_2 formed by the VUV photon was too low. Nevertheless there can hardly be any doubt that the reaction cycle 6 is taking place, given the known efficiency of its individual steps.

Analogous to the case of DME clusters, eqn (5) and (6) convincingly explain the extensive decay of HAc clusters after VUV excitation and the overwhelming dominance of mass peaks of protonated species in the resulting mass spectra. In contrast to the essentially thermoneutral decomposition of DME, that of HAc is markedly exothermic so that the cluster decay in the VUV mass spectra appears more pronounced for HAc clusters (Fig. 6) than for DME clusters (Fig. 5).

3.3 Case II: minor cluster decay after VUV ionization

H_2O clusters. The situation for H_2O and MeOH must be different from that of DME and HAc. The comparison with the Na-doped UV mass spectra in Fig. 3 and 4 shows that VUV excitation does here not result in extensive cluster fragmentation. The water and methanol ions undergo fast proton transfer processes that are analogous to those observed for DME and HAc, but there is evidently no analogous reaction cycle that could catalyze the subsequent decomposition of the cluster. This is most obvious for the H_2O clusters and has been extensively discussed and investigated in the literature (see Dong *et al.*,[2] Belau, *et al.*[3] and references therein).

$$H_2O^+ + H_2O \rightarrow H_3O^+ + OH \quad \Delta_rH \sim -1.01 \text{ eV} \qquad (7)$$

The hydroxyl radical formed by eqn (7) cannot trigger any exothermic or thermoneutral chain reaction in the clusters. It simply evaporates from the cluster after the fast proton transfer, leaving behind the protonated clusters detected in the mass spectrum. Even though the proton transfer releases $\sim$97 kJ mol^{-1} of energy it does not produce any significant cluster decay because of the substantial heat of vaporization of the bulk of $\Delta_{vap}H$ = 44.004 kJ mol^{-1}. If in addition all of the excess energy from the 13.3 eV photon ($\sim$0.7 eV = 68 kJ mol^{-1} relative to the monomer ionization energy) were available for evaporation, which is unlikely,[2] a maximum of 3–4 molecules could evaporate on average. One might argue that neither the bulk enthalpy of vaporization nor the ionization energy of the monomer is a particularly good approximation for the small protonated water clusters considered here. However, using cluster dissociation energies of small protonated clusters and cluster ionization energies (Dong *et al.*,[2] Belau *et al.*[3] and references therein) leads to similar results since both corrections go in opposite directions. Therefore, we think that the absence of intracluster chemistry beyond the proton transfer together with these simple estimates provide a good explanation why only a small difference is observed between VUV and Na-doping for water. (The VUV mass spectra show a minor shift to slightly smaller clusters compared to the UV mass spectra of the Na-doped clusters.) The same holds for the MeOH clusters which are discussed in the following.

MeOH clusters. In the case of MeOH clusters a catalytic decay would be conceivable, but it turns out to be energetically unfavourable. As a result the behaviour is similar to that of H_2O clusters so that the Na-doping mass spectrum and the VUV mass spectrum recorded for MeOH clusters at 13.3 eV look very similar (Fig. 3a and c). The proton transfer (eqn (8)) hardly provides enough energy (48 kJ mol^{-1}) to evaporate only a single molecules ($\Delta_{vap}H$ = 37 kJ mol^{-1}). Even if the whole photon excess energy were available in addition less than about 8 molecules could be evaporated.

$$CH_3OH^+ + CH_3OH \rightarrow CH_3OH_2^+ + CH_3O \quad \Delta_rH \sim -0.51 \text{ eV} \qquad (8)$$

Given the similarity of the Na-doping and VUV spectra there can be no significant additional chemical decay of the MeOH clusters after proton transfer. (Note again that the 10.1 eV mass spectrum cannot be used for comparison since this photon energy lies below the MeOH monomer ionization energy. See also comments in Section 3.1.) The only fragmentation of methanol that would result in stable volatile fragments is the dissociation into formaldehyde and hydrogen (eqn (9)).

$$CH_3OH = CH_2O + H_2 \quad \Delta_rH \sim +1.00 \text{ eV} \qquad (9)$$

Plausible catalytic cycles (eqn (9a) and (9b) or (9c) and (9d)) are carried by the methoxy radical after its initial formation in the proton transfer reaction (eqn (8)).

$$CH_3O \rightarrow HCO + H_2 \quad \Delta_rH \sim +0.27 \text{ eV} \qquad (9a)$$

$$HCO + CH_3OH \rightarrow CH_2O + CH_3O \quad \Delta_rH \sim +0.72 \text{ eV} \qquad (9b)$$

or

$$CH_3O \rightarrow CH_2O + H \quad \Delta_rH \sim +0.96 \text{ eV} \qquad (9c)$$

$$H + CH_3OH \rightarrow CH_3O + H_2 \quad \Delta_rH \sim +0.04 \text{ eV} \qquad (9d)$$

The fragmentation would consume approximately 96 kJ mol^{-1} per cycle. Assuming that the maximum possible energy of $\sim$286 kJ mol^{-1} ($\sim$3 eV) from the proton transfer and the photon excess energy at 13.3 eV relative to the monomer ionization energy were available, the reaction would stop after only three cycles. While the process is possible it would be irrelevant for major cluster destruction after VUV excitation, in full agreement with the experimental observations. The same arguments hold for the alternative decay into carbon monoxide and hydrogen (not shown here but analogous to eqn (4)), which would have practically the same energy balance.

The last point we would like to address here is the influence of the excess energy. In the case both of MeOH and of H_2O the VUV mass spectra obtained at 17.5 eV and 13.3 eV (Fig. 3 and 4) show similar cluster size distributions (somewhat obscured by

the lower signal to noise at 17.5 eV). This is a further indication that the excess energy does not play a major role for cluster decay. A plausible explanation is that the electron takes most of the excess energy.

4. Conclusions and outlook

The aim of the present paper was to study how intracluster reactions after single photon VUV ionization of weakly-bound clusters affect cluster fragmentation. To determine the degree of fragmentation, we used the Na-doping method as a reference. We have compared two classes of clusters: water and methanol clusters with ''minor ionic reactivity'' and dimethyl ether and acetic acid clusters with ''extensive ionic reactivity''. Upon VUV ionization, a fast proton transfer occurs in all four systems as a first step, which releases on the order of 0.4–1 eV energy. While essentially no further reactions occur in ionic water and methanol clusters, the proton transfer provides the initiators for the radical chain reactions in ionic dimethyl ether and acetic acid clusters. We believe that this explains why cluster fragmentation upon VUV ionization is only minor for water and methanol clusters, but extensive in the cases of dimethyl ether and acetic acid. The intracluster chain reactions lead to the successive decay of neutral dimethyl ether molecules and acetic acid molecules into small stable molecules. The volatile products easily escape from the clusters so that the chain reactions and the ensuing fragmentation are not immediately evident in the VUV mass spectra.

Our study shows that ionic chemistry after VUV ionization can play the dominant role for cluster fragmentation even at excitation energies close to the ionization threshold. Because of such potential intracluster reactions direct VUV ionization at threshold cannot in general be considered a soft ionisation method for such weakly-bound systems. Even at higher excitation energies, we found intracluster chemistry to be more important for fragmentation than the photon excess energy for the examples studied. The dimethyl ether and acetic acid example illustrate that intracluster reactions can go undetected in the mass spectra. At this point we cannot formulate a simple propensity rule for extensive cluster fragmentation by post-ionization reactions. The possibility, however, must clearly be taken into consideration whenever the break-up of the cluster's constituents into small stable product molecules is exothermic or approximately thermoneutral.

More generally, the present paper illustrates that for certain molecular aggregates the mass spectra recorded after direct ionization with minor excess energy are not even an approximate measure of the original cluster size distribution. This statement is not limited to VUV ionization, but also holds for other direct ionization methods, such as electron ionization. As pointed out in a previous publication, Na-doping largely avoids post-ionization chemistry so that it appears to offer a more accurate alternative for sizing weakly-bound clusters and ultrafine aerosols.[6] Independent cluster and aerosol sizing methods are crucial for any further size-dependent studies of such weakly-bound finite-sized systems.[35,36]

Acknowledgements

We thank Dr. David Luckhaus for help with the *ab initio* calculations. Financial support was provided by the Natural Sciences and Engineering Research Council of Canada (NSERC) and the Canada Foundation for Innovation. We acknowledge funding of two postdoctoral fellowships by the Swiss National Science Foundation (B.Y. and B.S.), of an NSERC graduate fellowship (J.L.), and of an NSERC E. W. R. Steacie Memorial Fellowship (R.S.).

References

1 P. Jena and A. W. Castleman Jr., *Proc. Natl. Acad. Sci. U. S. A.*, 2006, **103**, 10560–10569.
2 F. Dong, S. Heinbuch, J. J. Rocca and E. R. Bernstein, *J. Chem. Phys.*, 2006, **124**, 224319.
3 L. Belau, K. R. Wilson, S. R. Leone and M. Ahmed, *J. Phys. Chem.*, 2007, **111**, 10075–10083.
4 Y. J. Hu, H. B. Fu and E. R. Bernstein, *J. Chem. Phys.*, 2006, **125**, 184308.
5 S. Wei, W. B. Tzeng and A. W. Castleman Jr., *J. Phys. Chem.*, 1991, **95**, 5080–5085.
6 B. L. Yoder, J. H. Litman, P. W. Forysinski, J. L. Corbett and R. Signorell, *J. Phys. Chem. Lett.*, 2011, **2**, 2623–2628.
7 S. Schütte and U. Buck, *Int. J. Mass Spectrom.*, 2002, **220**, 183–192.
8 C. Bobbert, S. Schütte, C. Steinbach and U. Buck, *Eur. Phys. J. D*, 2002, **19**, 183–192.
9 P. W. Forysinski, P. Zielke, D. Luckhaus, J. Corbett and R. Signorell, *J. Chem. Phys.*, 2011, **134**, 094314.
10 L. Cwiklik, U. Buck, W. Kulig, P. Kubisiak and P. Jungwirth, *J. Chem. Phys.*, 2008, **128**, 154306.
11 H. T. Liu, J. P. Müller, N. Zhavoronkov, C. P. Schulz and I. V. Hertel, *J. Phys. Chem.*, 2010, **114**, 1508–1513.
12 P. W. Forysinski, P. Zielke, D. Luckhaus and R. Signorell, *Phys. Chem. Chem. Phys.*, 2010, **12**, 3121–3130.
13 *NIST Chemistry WebBook, NIST Standard Reference Database Number 69*, ed. P. J. Linstrom and W. G. Mallard, National Institute of Standards and Technology, Gaithersburg MD, 20899, http://webbook.nist.gov (retrieved August 2012).
14 E. D. Skakovskii, S. A. Lamotkin and L. Y. Tychinskaya, *J. Appl. Spectrosc.*, 1997, **64**, 319–324.
15 Z. Lu and R. E. Continetti, *J. Phys. Chem.*, 2004, **108**, 9962–9969.
16 A. Fraind, R. Turncliff, T. Fox, J. Sodano and L. R. Ryzhkov, *J. Phys. Org. Chem.*, 2011, **24**, 809–820.
17 N. S. Shuman, W. R. Stevens and T. Baer, *Int. J. Mass Spectrom.*, 2010, **294**, 88–92.
18 J. C. Traeger, R. G. McLoughlin and A. J. C. Nicholson, *J. Am. Chem. Soc.*, 1982, **104**, 5318–5322.
19 Z. Shi, J. V. Ford, S. Wei and A. W. Castleman Jr., *J. Chem. Phys.*, 1993, **99**, 8009–8015.
20 Y.-S. Wang, C.-H. Tsai, Y. T. Lee, H.-C. Chang, J. C. Jiang, O. Asvany, S. Schlemmer and D. Gerlich, *J. Phys. Chem.*, 2003, **107**, 4217–4225.
21 E. P. Grimsrud and P. Kebarle, *J. Am. Chem. Soc.*, 1973, **95**, 7939–7943.
22 K. A. G. Macneil and R. N. Dixon, *J. Electron Spectrosc. Relat. Phenom.*, 1977, **11**, 315–331.
23 F. Merkt, R. Signorell, H. Palm, A. Osterwalder and M. Sommavilla, *Mol. Phys.*, 1998, **95**, 1045–1054.
24 J. J. Butler, D. M. P. Holland, A. C. Parr and R. Stockbauer, *Int. J. Mass Spectrom.*, 1984, **58**, 1–14.
25 P. Zielke, P. W. Forysinski, D. Luckhaus and R. Signorell, *J. Chem. Phys.*, 2009, **130**, 211101.
26 O. Kostko, L. Belau, K. R. Wilson and M. Ahmed, *J. Phys. Chem. A*, 2008, **112**, 9555–9562.
27 M. Faubel, B. Steiner and J. P. Toennies, *J. Chem. Phys.*, 1997, **106**, 9013–9031.
28 B. Winter, R. Weber, W. Widdra, M. Dittmar, M. Faubel and I. V. Hertel, *J. Phys. Chem. A*, 2004, **108**, 2625–2632.
29 F. Carnovale, T. H. Gan and J. B. Peel, *J. Electron Spectrosc. Relat. Phenom.*, 1980, **20**, 53–67.

30 M. J. Frisch, G. W. Trucks, H. B. Schlegel, G. E. Scuseria, M. A. Robb, J. R. Cheeseman, G. Scalmani, V. Barone, B. Mennucci, G. A. Petersson, H. Nakatsuji, M. Caricato, X. Li, H. P. Hratchian, A. F. Izmaylov, J. Bloino, G. Zheng, J. L. Sonnenberg, M. Hada, M. Ehara, K. Toyota, R. Fukuda, J. Hasegawa, M. Ishida, T. Nakajima, Y. Honda, O. Kitao, H. Nakai, T. Vreven, J. A. Montgomery Jr., J. E. Peralta, F. Ogliaro, M. Bearpark, J. J. Heyd, E. Brothers, K. N. Kudin, V. N. Staroverov, R. Kobayashi, J. Normad, K. Raghavachari, A. Rendell, J. C. Burant, S. S. Iyengar, J. Tomasi, M. Cossi, N. Rega, J. M. Millam, M. Klene, J. E. Knox, J. B. Cross, V. Bakken, C. Adamo, J. Jaramillo, R. Gomperts, R. E. Stratmann, O. Yazyev, A. J. Austin, R. Cammi, C. Pomelli, J. W. Ochterski, R. L. Martin, K. Morokuma, V. G. Zakrzewski, G. A. Voth, P. Slavador, J. J. Dannenberg, S. Dapprich, A. D. Daniels, Ö. Farkas, J. B. Foresman, J. V. Oritz, J. Cioslowski and D. J. Fox, *Gaussian, Inc.*, Wallingford CT, 2009.
31 Y. Gong and L. Andrews, *J. Phys. Chem. A*, 2011, **115**, 3029–3033.
32 D. A. Good and J. S. Francisco, *J. Phys. Chem.*, 2000, **104**, 1171–1185.
33 J.-y. Liu, Z.-s. Li, J.-y. Wu, Z.-g. Wei, G. Zhang and C.-c. Sun, *J. Chem. Phys.*, 2003, **119**, 7214–7221.
34 Z. Zhao, M. Chaos, A. Kazakov and F. L. Dryer, *Int. J. Chem. Kinet.*, 2008, **40**, 1–18.
35 B. L. Yoder, A. West, B. Schläppi, E. Chasovskikh and R. Signorell, 2012, submitted.
36 J. Fedor, J. Kočišek, V. Poterya, O. Votava, A. Pysanenko, M. L. Lipciuc, T. N. Kitsopoulos and M. Fárník, *J. Chem. Phys.*, 2011, **134**, 154303.